

Observation of a Laser-Assisted Ionization of the $\text{He}(2^1S, 2^3S) + \text{He}(1^1S)$ Collision System Involving a Bound-Free Transition

P. Pradel, P. Monchicourt, D. Dubreuil, J. Heuze, J. J. Laucagne, and G. Spiess
*Service de Physique des Atomes et des Surfaces, Centre d'Etudes Nucleaires de Saclay,
 F-91191 Gif-sur-Yvette Cedex, France*

(Received 26 November 1984)

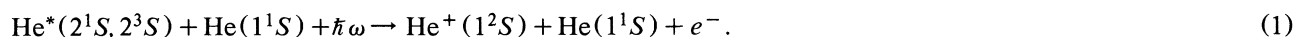
We report the first observation of an assisted He^+ yield arising from single collisions between a $\text{He}(2^1S, 2^3S)$ atom beam on a $\text{He}(1^1S)$ target in the presence of an intense laser field. A time-of-flight analysis shows that the pulsed laser-assisted ion signal is reproducible, energy dependent, and appears in addition to the continuous ion flux coming from a known field-free diabatic channel. From the estimated value of the diabatic ionization cross section σ_d , the order of magnitude of the assisted-ionization cross section σ_a is given.

PACS numbers: 34.50.Rk, 34.50.Gb

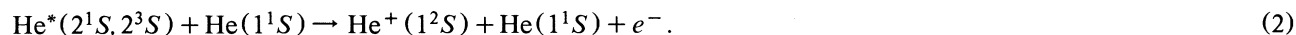
Laser-assisted collisions can be defined¹ as processes where photon absorption—or emission—is made possible only in the course of a collision between two atoms, whereas it is not possible when these two atoms are far apart. Besides the interest for laser-switched reactions, such processes are of fundamental importance because they allow the study of the optical properties of transient molecules, i.e., the modification of the electron structure of two interacting atoms. Experimental evidence is now clearly established for bound-bound transitions,² where the resonant nature of the process allows high cross sections and pressure-broadening spectroscopy.³ These two major features are absent for bound-free transitions. It is, therefore, much more difficult to realize them experimentally,

since field-free ionizing processes can compete, especially in high-density-cell or thermal-beam experiments.⁴ As a result of these competing processes,⁵ it seems necessary to provide the first experimental evidence of laser-assisted ionization by use of a simple dynamical collision system. This would be the opportunity to test the existing theory of laser-induced processes.⁶

A low-density-beam experiment with angular and time-of-flight analysis of the produced ions allows the selective study of such a process. We present here results giving the first direct and clear evidence of a laser-assisted nonresonant ionizing collision, together with its order-of-magnitude cross section. The investigated bound-free assisted process is



The metastable states $\text{He}^*(2^1S)$ and $\text{He}^*(2^3S)$ lie respectively 4 and 4.8 eV below He^+ . The photon energy $\hbar\omega = 3.49$ eV is chosen so as not to be resonant with any atomic transition, and to avoid direct photoionization of He^* . The $\text{He}(1^1S)$ atom acts only as a perturber which shifts the He^* levels and allows photon absorption. In Fig. 1 are plotted the well-known potential curves of the $\text{He}^* + \text{He}$ and He_2^+ systems,^{7,8} together with the relevant field-dressed curves for one-photon absorption. Ionization becomes possible when the $2^1\Sigma_g$ and $2^3\Sigma_g$ field-dressed curves penetrate the $\text{He}^+ + \text{He} + e^-$ continuum. This occurs at $R < 2.25$ Å for the singlet, and $R < 1.94$ Å for the triplet. The low density of the beam ($< 10^3$ cm⁻³) avoids $\text{He}^* - \text{He}^*$ collisions. Ion signals have been obtained for two kinetic energies of the beam, 50 and 35 eV in the center-of-mass system, i.e., 100 and 70 eV in the laboratory. In this energy range, field-free collisional ionization is possible via a diabatic nonresonant channel⁹ (see Fig. 1):



The value of σ_d derived from Ref. 9 allows a calibration of σ_a by direct comparison between the two ion signals.

A part of the experimental apparatus has been described in detail elsewhere.¹⁰ Briefly a 500-eV He^+ beam is extracted from a Colutron source, focused by a cylindrical lens, and decelerated to the working energy. The He^* beam comes from He^+ beam neutralization via quasiresonant charge-transfer reactions on a cesium target.¹¹ The remaining charged particles are removed from the beam by a transverse electric field.

The He^* beam enters the He-gas-target cell, 12 mm long, through two collimating apertures (see Fig. 2). A Westinghouse ionization gauge is used to monitor the target-gas pressure during the experiments; it was verified that this pressure ensured single-collision conditions. He^+ resulting from Reaction (1) or (2)⁹ and residual neutral atoms scattered in a θ_L direction defined by two rectangular slits of dimensions 0.9×4 mm² drift through a field-free region and afterwards are charge analyzed by a transverse electric field; the

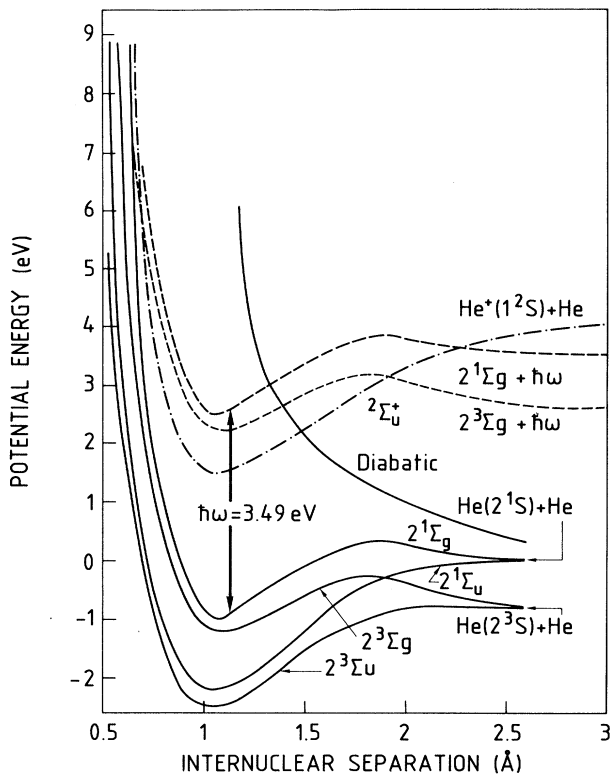


FIG. 1. Relevant adiabatic potential curves of He_2^* and He_2^+ obtained with use of Refs. 7 and 8. The diabatic curve correlated with the $\text{He}(2^1S) + \text{He}$ level is drawn from Ref. 7. Broken lines represent the field-dressed potential curves.

separated ions are then incident on a Channeltron. In this Letter we report only measurements for zero scattering angle where the ion signals present the best statistics. The He^* beam is crossed with an orthogonal laser light beam in the interaction chamber. The assistance radiation is the third harmonic of a commercial (Moletron MY 33) Nd-doped yttrium aluminum gar-

net laser ($\lambda = 355 \text{ nm}$), which routinely delivers 20-mJ light pulses with 20-nsec duration time and 10-Hz repetition rate. In order to illuminate all of the collision volume a telescope is used to give a parallel beam of section $\sim 12 \times 2 \text{ mm}^2$ where the average power density is $\sim 10 \text{ MW/cm}^2$. The ions produced during the laser pulse via the assisted process (1) are superimposed on the background diabatic signal from Reaction (2). At 50 eV, all of these ions reach the detector after a time of flight of $4.1 \mu\text{sec}$ (4.9 at 35 eV). Output counting pulses from the Channeltron are amplified and fed simultaneously into a fast multichannel analyzer and a counter which acts as an ion monitor. In order to distinguish the assisted ions from the diabatic background, the analyzer is activated about $1 \mu\text{sec}$ before the arrival of the assisted ions and scans 50 channels, each 50 nsec in duration.

Figure 3 shows the histograms of the data. Each histogram is taken with the same number of laser shots and the same irradiation conditions. The experimental conditions were as follows: (a) For $E_{c.m.} = 50 \text{ eV}$, metastable beam density $N^* \sim 8.6 \times 10^2 \text{ atoms cm}^{-3}$; unfocused average light power density $I \sim 8 \times 10^6 \text{ W cm}^{-2}$; He target density $\sim 1.6 \times 10^{12} \text{ atoms cm}^{-3}$. (b) For $E_{c.m.} = 35 \text{ eV}$, $N^* \sim 4.8 \times 10^2 \text{ atoms cm}^{-3}$; the other parameters remaining identical. From these conditions the background count rate for the diabatic signal (at 50 eV with laser off) was $\sim 400 \text{ ions sec}^{-1}$. Combining the He^* -atom crossing time through the cell, the laser pulse duration, the time-of-flight uncertainty, and the beam-energy-spread effect, the assisted ions are expected in a window containing seven channels (350 nsec). For $E_{c.m.} = 50 \text{ eV}$, we see inside this window a laser-correlated ion-contribution peak which is equal to the diabatic signal. In the same way for $E_{c.m.} = 35 \text{ eV}$, the window signal peak is 2.5 times larger than the diabatic one. As the He^* -atom crossing time through the 12-mm cell is ten times larger than the laser pulse duration at $E_{c.m.} = 50 \text{ eV}$, we

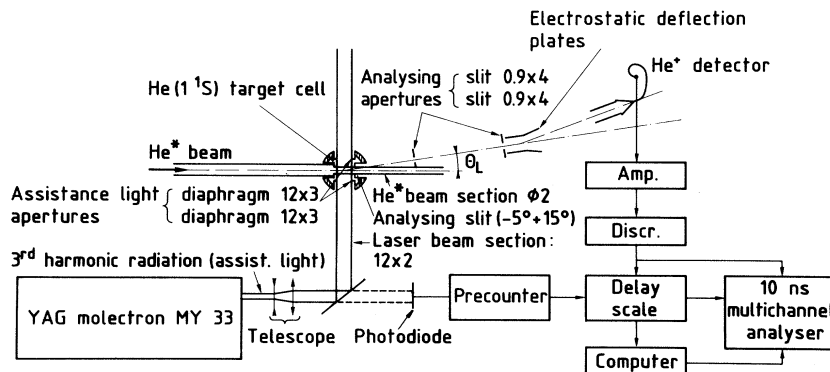


FIG. 2. Schematic view of the experimental setup showing the interaction region and the detection system. The drawing is not to scale. Dimensions are in millimeters. Measurements have been performed for $\theta_L = 0$.

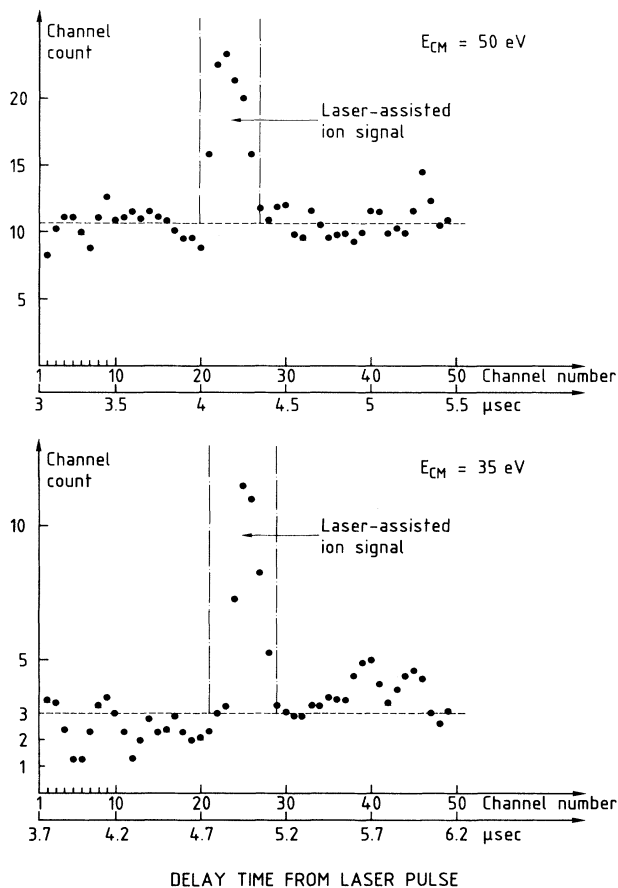


FIG. 3. Diabatic- and assisted-signal histogram for $E_{c.m.} = 50$ eV and $E_{c.m.} = 35$ eV. Expected assisted-signal window is shown by vertical dash-dotted lines. The horizontal dashed lines represent the averaged value of the pure diabatic signal (outside the window). Note that the contrast between the two kinds of ions is more important when collision energy decreases.

deduce from these ion-signal magnitudes that for $I \sim 8 \times 10^6$ W cm $^{-2}$, $\sigma_a \sim 10\sigma_d$ ($\sigma_a \sim 29\sigma_d$ for $E_{c.m.} = 35$ eV). From the $2^3S \rightarrow 2^3P$ transition probability given by Gillen, Peterson, and Olson,⁹ we estimate the lower limit of the diabatic cross section for $E_{c.m.} = 50$ eV: We find $\sigma_d > 4 \times 10^{-19}$ cm 2 and therefore $\sigma_a > 4 \times 10^{-18}$ cm 2 . In agreement with Ref. 9, σ_d increases with increasing energy, by a factor 1.7 ± 0.1 in this energy range; on the contrary, σ_a decreases by a factor 0.6 ± 0.6 , showing that, within these experimental uncertainties the colliding system exhibits a completely different kinematics when illuminated by laser light. We have checked the linear dependence of σ_a vs the average light power density I by working at $I/2$: The resulting assisted ion signal is reduced by a factor of 2.2 which is very satisfactory in view of our statistics. Each histogram takes 5.4×10^5 laser shots leading to an overall counting time of about

seventeen hours.

The laser-assisted channel (1) is the only process consistent with our observations. We have verified that the assisted signal disappears when removing either the laser beam, or the He target, or the bias on the electrostatic deflection plates. The following competing reactions cannot account for the additional ion contribution measured in the window.

(1) Two-photon ionization of He*: This process does not need the presence of the He target, whereas our ion signal disappears when the He target is removed.

(2) Photoexcitation of He*, followed by collisional ionization: A two-step process is not allowed, because $\hbar\omega$ is not resonant with any atomic transition (energy defect ≥ 0.1 eV). However, photoexcitation may occur during the collision, when the photon becomes resonant with the $2\Sigma \rightarrow n\Pi$ transitions of the transient He $_2$ molecule ($6 \leq n < \infty$ from $2^1\Sigma$, and $4 \leq n < \infty$ from $2^3\Sigma$). Ions may be subsequently produced.¹² By use of standard atomic oscillator strengths for these optical transitions,¹³ laser-assisted Landau-Zener cross sections,¹⁴ and summation of the contribution for each transition, a total cross section of less than 6×10^{-21} cm 2 is obtained. This is 3 orders of magnitude smaller than what we observe.

(3) Collisional excitation of He*, followed by photoionization: Field-free He* + He inelastic collisions may produce higher excited states, which can be photoionized during the laser pulse. A Landau-Zener treatment with radial coupling elements calculated by Cohen¹² gives cross sections smaller than 10^{-19} cm 2 for excitation of $n \geq 3$ levels. The most probable contributing process is $2^1S \rightarrow 2^1P$ excitation (energy defect = 0.6 eV), followed by photoionization. There is no triplet contribution since the 2^3P cannot be photoionized by a 3.49-eV photon. In this two-step reaction, ion production has to increase with kinetic energy.^{9,15} As shown in Fig. 3, we observe the opposite effect. Hence, this is a strong indication that we observe a laser-assisted process, and not a two-step mechanism. In order to get a more convincing demonstration, a complementary experiment has been performed, by use of a pure He*(2^3S) beam instead of a mixed ($2^1S + 2^3S$) one. This pure, but less dense beam has been obtained at $E_{c.m.} = 50$ eV by replacement of the Cs of the charge-exchange cell by Na.¹⁶ In this case, the contribution from 2^1P and 2^3P photoionization is completely removed. Since the ion signal is still present, we conclude that it can only be produced by a laser-assisted process. The observed increase of σ_a with decreasing kinetic energy (see Fig. 3) is in agreement with such a process, since laser-assisted cross sections are expected to increase with the collision time.

Helpful discussions with T. F. George and J. S.

Cohen are gratefully acknowledged. This work was partially supported by the Direction des Recherches Etudes et Techniques under Contract No. 81 34 170 00 470 7501.

¹L. I. Gudzenko and S. I. Yakovlenko, Zh. Eksp. Teor. Fiz. **62**, 1686 (1972) [Sov. Phys. JETP **35**, 877 (1972)].

²R. W. Falcone, W. R. Green, J. C. White, J. F. Young, and S. E. Harris, Phys. Rev. A **15**, 1333 (1977).

³A. Gallagher and T. Holstein, Phys. Rev. A **16**, 2413 (1977); C. Brechignac, Ph. Cahuzac, and P. E. Toschek, Phys. Rev. A **21**, 1969 (1980).

⁴J. Boulmer and J. Weiner, Phys. Rev. A **27**, 2817 (1983), and references therein.

⁵J. Huennekens and A. Gallagher, Phys. Rev. A **27**, 771 (1983).

⁶J. C. Bellum and T. F. George, J. Chem. Phys. **70**, 5059 (1979); S. Geltman, J. Phys. B **10**, 3057 (1977).

⁷R. P. Saxon, K. T. Gillen, and B. Liu, Phys. Rev. A **15**, 543 (1977).

⁸S. L. Guberman and W. A. Goddard, III, Phys. Rev. A **12**, 1203 (1975).

⁹K. T. Gillen, J. R. Peterson, and R. E. Olson, Phys. Rev. A **15**, 527 (1977).

¹⁰P. Pradel, M. El Maddarsi, and A. Valance, J. Phys. B **14**, 541 (1981).

¹¹P. Pradel and J. J. Laucagne, J. Phys. (Paris) **44**, 1263 (1983).

¹²J. S. Cohen, Phys. Rev. A **13**, 86 (1976).

¹³W. L. Wiese, M. W. Smith, and B. M. Glennon, *Atomic Transition Probabilities*, U. S. National Bureau of Standards, National Standards Reference Data Series—4 (U.S. GPO, Washington, D. C., 1966), Vol. 1.

¹⁴S. I. Yakovlenko, Sov. Phys. J. Quantum Electron. **8**, 151 (1978).

¹⁵S. A. Evans, J. S. Cohen, and N. F. Lane, Phys. Rev. A **4**, 2235 (1971). The cross-section values of Table I should be read in units of $10^{16}a_0^2$ instead of square centimeters. E. J. Shipsey, J. C. Browne, and R. E. Olson, Phys. Rev. A **11**, 1334 (1975).

¹⁶C. Reynaud, J. Pommier, V. N. Tuan, and M. Barat, Phys. Rev. Lett. **43**, 579 (1979).